High p$_T$ EWK and QCD in CMS

Anne-Marie Magnan for the CMS Collaboration

Imperial College, Prince Consort Road, London SW7 2BW, United Kingdom

The LHC has been delivering data to CMS at a centre-of-mass energy of 7 TeV since April 2010, with an instantaneous luminosity that has been constantly increasing from 10^{27} to 10^{31} cm^{-2}s^{-1}. Both the machine and the detector have given outstanding performance. The detector community has been very fast to deliver physics results, which have already extended the transverse momentum reach of the Tevatron. This review will concentrate on preliminary results obtained with between 60 nb^{-1} and 1.7 pb^{-1} of data: inclusive jet and dijet production, 3-jet to 2-jet ratio, W/Z boson decays into leptons including W+jets and first observation of taus, and top quark studies in the dilepton and lepton+jet channels.

1 Introduction

QCD processes constitute the dominant source of interactions at the LHC due to their large cross sections relative to other processes [1]. This makes QCD an attractive topic for early physics at LHC. Several orders of magnitude lower in cross section are the electroweak (EWK) processes, with the W, Z and $t\bar{t}$ inclusive cross sections expected respectively at about 300 nb, 90 nb and 0.16 nb. By measuring jets and leptons, several objectives can be attained, both from the theoretical and experimental points of view: commissioning of the detectors, reconstruction of well-defined candles, verification of perturbative QCD (pQCD) at the TeV scale, tests of PDF evolution, probes of α_S, understanding of multijet production (as a background to other searches), and sensitivity to new physics.

The CMS detector is similar to other multi-purpose collider detectors. The central feature of the CMS apparatus is a superconducting solenoid, of 6 m internal diameter, providing a field of 3.8 T. Within the field volume are the silicon pixel and strip tracker, the lead-tungstate crystal electromagnetic calorimeter (ECAL) and the brass-scintillator hadronic calorimeter (HCAL). Muons are measured in gas chambers embedded in the iron return yoke. CMS also has extensive forward calorimetry, extending the pseudo-rapidity coverage of the calorimeters from $|\eta| > 3$ to $|\eta| < 5$. The ECAL has an energy resolution of about 0.5 % at 100 GeV. The HCAL, when combined with the ECAL, measures jets with a resolution $\Delta E/E \approx 100\,\%/\sqrt{E} \oplus 5\,\%$. The inner tracker measures charged particles within the $|\eta| < 2.5$ pseudo-rapidity range. More details can be found at [2].

The first level (L1) of the CMS trigger system, composed of custom hardware processors, uses information from the calorimeters and muon detectors to select, in less than 1 μs, the most interesting events (only one bunch crossing in 1000). The High Level Trigger (HLT) processor farm further decreases the event rate from 100 kHz to 100 Hz, before data storage.

The LHC has been delivering proton-proton collisions at a centre-of-mass energy of 7 TeV since March 29th, 2010. The constantly increasing luminosity lead to a doubling of the physics

dataset every week on average. A total integrated luminosity of $3.63\,\mathrm{pb}^{-1}$ was delivered to CMS by the end of August. These proceedings review physics results for integrated luminosities ranging from 60 nb^{-1} up to 1.7 pb^{-1} [3], as presented at the ISMD conference.

2 Jets and QCD measurements

Four different jet algorithms have been developed and are being used. The baseline clustering algorithm for all of them uses the infrared- and collinear-safe anti-k_T scheme [4], with a size of 0.5.

Calorimeter-based jets, or Calojets [5], use only calorimeter towers, and typically have energy resolution $\sigma_{p_T}/p_T \simeq 25\%$ at $30\,\mathrm{GeV}$ down to 5% at $1\,\mathrm{TeV}$, in the central rapidity region. The corresponding transverse missing energy is referred to as CaloMET.

Track-corrected jets, or Jet-Plus-Track (JPT) [6], are Calojets complemented with track information to improve the measurement. With 60% of the energy of a jet coming from charged particles, the gain in jet energy scale and resolution is important, particularly at low transverse momentum p_T where the tracker resolution is much better: $\sigma_{p_T}/p_T \simeq 15\%$ at $30\,\mathrm{GeV}$, 10% at $100\,\mathrm{GeV}$, joining up with Calojets at $1\,\mathrm{TeV}$, in the central region. Outside the tracker acceptance ($|\eta| > 2.5$), they are identical to Calojets. The corresponding transverse missing energy is referred to as tcMET.

Particle Flow (PF) jets are derived from a more complete reconstruction of the events using a particle flow algorithm [7], making use of both iterative tracking and calorimeter clustering using calibrated clusters. An additional gain in jet energy scale and resolution is obtained at low p_T, with $\sigma_{p_T}/p_T \simeq 12\%$ at $30\,\mathrm{GeV}$; the resolution approaches that of JPT jets at $100\,\mathrm{GeV}$, in the central region. The corresponding transverse missing energy is referred to as PFMET.

Track jets use only track information, and are described in more detail elsewhere [8].

The jet energy calibration is derived from Monte Carlo (MC) [5]. A first cross check with data indicates good agreement within the 10% (5%) uncertainties for Calo (JPT/PF) jets, with an additional uncertainty on the pseudo-rapidity dependence of $2\% \times |\eta|$. Comparison between data and MC in the dijet asymmetry analysis [5] sets the uncertainty on the jet energy resolution at 10%. Missing transverse energy reconstruction and calibration are discussed in detail elsewhere [9].

In all jet analyses, events are selected using minimum bias triggers (for the low luminosity data sample) and single-jet triggers, based on the selection of calorimeter trigger towers above thresholds of 6, 15, 30 or 50 GeV (uncorrected E_T). The threshold on the corrected p_T necessary to have 100% efficient selection using the 15 GeV trigger depends on the reconstruction algorithm: 32, 38 and 56 GeV, respectively for Calo, JPT and PF jets.

Figure 1: Impact of the systematic uncertainties on the inclusive jet cross section as a function of p_T.

All three jet types described above are used for the inclusive jet cross section measurement [10]. In addition to commissioning these objects for other analyses, it is also important to demonstrate that the systematic uncertainties are well understood. The main systematics are
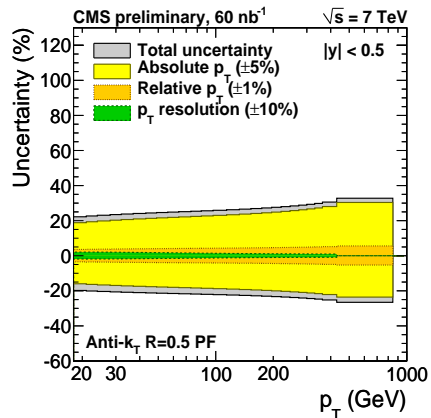
shown in Fig. 1 as a function of p_T for the PF jets. Similar uncertainties are obtained for JPT jets, but for Calojets, the impact of the absolute scale should be doubled ($\pm 10\%$ as described above). The event selection rejects beam background by requiring at least one good vertex, and at least 25% good quality tracks. Data are corrected back to the hadron-level using the 'Ansatz method' developed at the Tevatron [11]. The correction factor is found to vary between 80 and 95% as p_T increases. NLO predictions are extracted using NLOJet++ and fastNLO [12]. Nonperturbative corrections are derived by comparing Pythia and Herwig++ predictions, and correspond to a correction factor of 1.3 at 30 GeV, down to close to 1 above 100 GeV [10] for rapidity $|y| < 0.5$. The
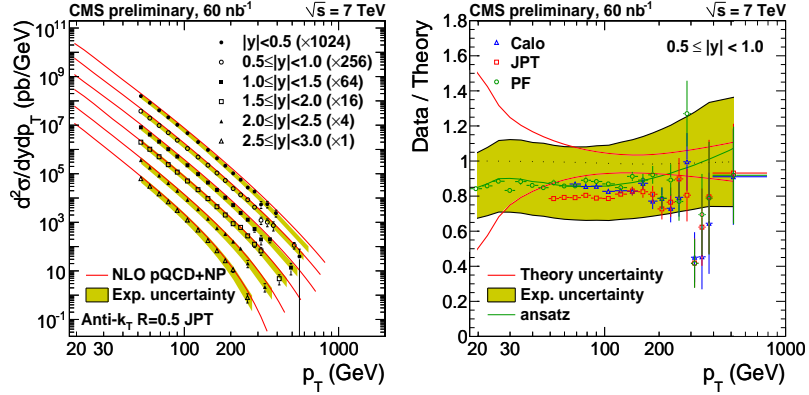

Figure 2: Inclusive cross section as a function of p_T and rapidity (left) and Data/Theory ratios as a function of p_T for $0.5 < |y| < 1.0$ (right).

final spectra after selection of jets with $p_T > 50$ GeV and for the six rapidity regions considered in this analysis are shown in Fig. 2 (left), for JPT jets, with $60\,\mathrm{nb}^{-1}$ of integrated luminosity. Ratios between data and NLO predictions are shown for the three algorithms studied in Fig. 2 (right) for $0.5 < |y| < 1.0$. Within the systematic uncertainties, all three algorithms are in good agreement with NLO predictions.

Using similar data selection, the dijet mass spectrum is shown in Fig. 3 (left) for Calojets with a cone size of 0.7, for $120\,\mathrm{nb}^{-1}$ of integrated luminosity. The agreement with Pythia simulation is very good, and preliminary limits on new phenomena models that are the world's best have been derived [13].
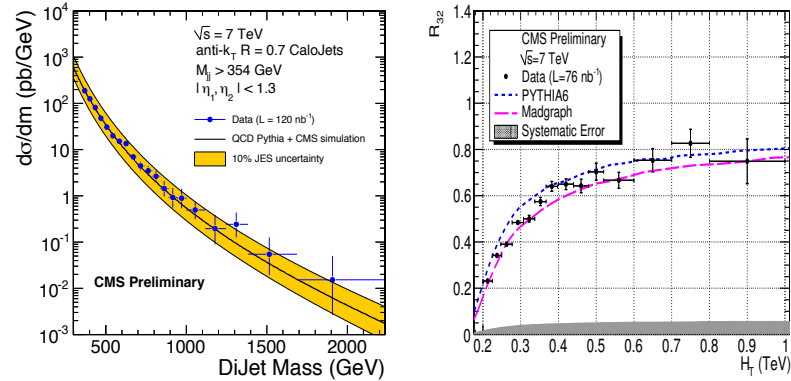

Figure 3: Dijet mass spectrum (left) and 3-jet to 2-jet ratio (right).

Another important measurement concerns the 3-jet to 2-jet ratio [14]. The characteristic quantity is $R_{32} = \frac{d\sigma_3/dH_T}{d\sigma_2/dH_T}$, which has a plateau at high H_T sensitive to α_S. This ratio is shown as a function of H_T in Fig. 3 (right) for $76\,\mathrm{nb}^{-1}$ of integrated luminosity.

CMS results with p-p collisions at 7 TeV confirm pQCD predictions, with the available statistics and within systematic uncertainties. Matrix element and parton shower generators

give a very good description of the data.

3   Leptons and EWK measurements

The main ingredients of measurements based on final states with high-p_T leptons are identification of one or more isolated leptons, data-driven methods to extract the background shapes, and likelihood fits to extract the signal yields.

Electron identification is based on track-cluster association and cluster width variables, with cuts optimised for selection efficiency [15]. For measurements of the Z, a 95% (loose) efficient selection is used, while for W and $t\bar{t}$, a 75% (tight) efficient selection is required. To identify muons, good consistency between inner tracker and muon chamber measurements is required [16]. Low p_T resonances in $\mu^+\mu^-$ are extremely well-resolved, in particular Υ^{1s}, Υ^{2s} and Υ^{3s} [17]. Events are selected using single lepton triggers, with thresholds of 15 (9) GeV for electrons (muons). These triggers are fully efficient for leptons with reconstructed $p_T > 20$ GeV.

The shape of the multijet background is taken from data using a sample with inverted isolation; other EWK and signal shapes are taken from simulation. The W yield is extracted using a binned likelihood fit to the transverse mass distribution between the electron and the PFMET. The Z yield is obtained by simply counting the number of events remaining after the selection, as the background contribution is shown to be negligible.

The cross sections measured for W and Z production are shown in Fig. 4 for the electron and muon channels, along with the NNLO predictions. All measurements are compatible with the theory when considering the luminosity uncertainty of 11% (shown separately as the green error band). Transverse mass and dilepton invariant mass distributions, and other cross section measurements like the W^+/W^- ratio, are shown in more detail elsewhere [18].
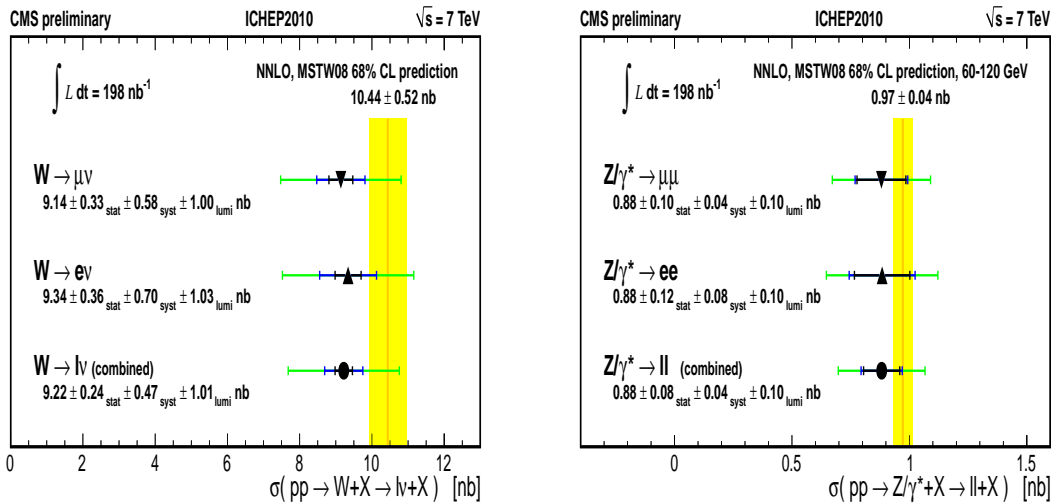

Figure 4: $pp \rightarrow W + X \rightarrow l\nu + X$ (left) and $pp \rightarrow Z + X \rightarrow ll + X$ (right) cross section measurements.

The W charge asymmetry deserves more attention, however, as it is particularly relevant in p-p collisions. Measurement of the lepton asymmetry, defined as $A(\eta) = \frac{d\sigma^+/d\eta - d\sigma^-/d\eta}{d\sigma^+/d\eta + d\sigma^-/d\eta}$, provides a handle on the quark content of the proton, and is sensitive to new physics [18]. This quantity is shown in Fig. 5 (left) as a function of lepton pseudo-rapidity, for both electron and muon channels.
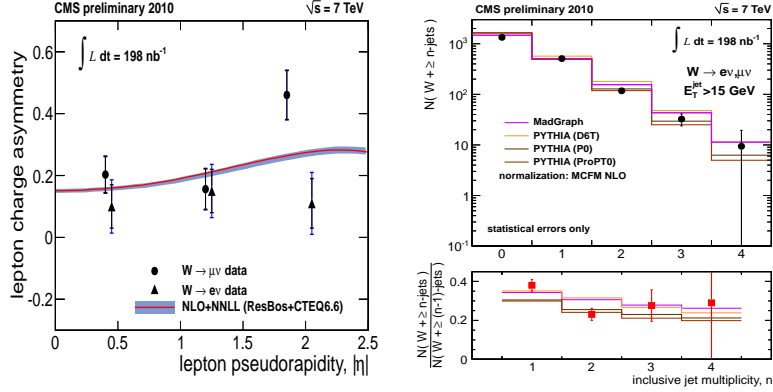

Figure 5: Lepton charge asymmetry as a function of pseudo-rapidity (left). Ratio of W events in consecutive multiplicity bins (right).

The standard model predicts a value $A(\eta) \simeq 0.2 \pm 0.04(PDF)$. With $10\,\mathrm{pb}^{-1}$, the measurement uncertainty is expected to be smaller than the theoretical one, and hence put constraints on PDF models.

First measurements of jet multiplicity in W events have also been performed [18]. This measurement is aimed at constraining pQCD predictions, but is also sensitive to new physics. PF jets are used with $|\eta| < 2.5$. The ratio of W events in each multiplicity bin $\frac{N(W + \geq n-jets)}{N(W + \geq (n-1)-jets)}$ has been studied for jets with E_T threshold of 15 and 30 GeV. The rate of jets in data is compared to different Pythia tunes at low p_T, as shown in Fig. 5 (right), and to two different generators, Pythia and Madgraph, at high p_T.

Even though they are not as efficiently reconstructed as electrons or muons, first taus from Z bosons are already available [19]. The efficiency of the PF-based tau identification algorithms used is currently extracted from MC with 60% efficiency for a visible $\mathrm{p}_T > 50\,\mathrm{GeV}$. The rate of fakes, which come mainly from multijet and W processes, has been measured in data in a sample of $8.4\,\mathrm{nb}^{-1}$ of integrated luminosity, and found to be around

Figure 6: Visible mass of the $\mu\tau^{had}$ pair, with $\mathrm{p}_T^\mu > 15\,\mathrm{GeV}$ and $\mathrm{p}_T^\tau > 20\,\mathrm{GeV}$ (left). Number of b-tagged jets after the dilepton selection (right).

1%. The visible mass in the decay channel $Z \rightarrow \tau\tau \rightarrow \mu\tau^{had}$, with $\mathrm{p}_T^\mu > 15\,\mathrm{GeV}$ and $\mathrm{p}_T^\tau > 20\,\mathrm{GeV}$ is shown in Fig. 6 (left), for $1.7\,\mathrm{pb}^{-1}$ of integrated luminosity.

The last measurements covered in these proceedings concern the selection of $t\bar{t}$ events in the dilepton and lepton+jets channels [20]. These measurements demonstrate the excellent performance of the CMS detector, and of the reconstruction of leptons and jets. Also important is heavy-flavour tagging in the identification of signal events [21]. JPT jets are used in the dilepton channel, and Calojets in the lepton+jet channel, with $p_T > 30\,\mathrm{GeV}$. A track-counting b-tag algorithm is used, with a b-tag efficiency of 81% and a mis-tag efficiency of 10% for charm and light jets. The number of b-tagged jets after the dilepton selection is shown in Fig. 6 (right). For $0.84\,\mathrm{pb}^{-1}$ of integrated luminosity, the dilepton selection yields four candidates in the data for a relatively pure signal yield expected from MC. More information, and the measurement of the cross section which has been published since the ISMD conference, can be found at [20].

4 Conclusion

With the currently available statistics, and within experimental uncertainties, CMS is already in a good position to confirm the standard model predictions for the first QCD and EWK measurements in p-p collisions at $7\,\mathrm{TeV}$. Preliminary limits which are the world's best are extracted in some new physics models, the momentum reach has exceeded that of the Tevatron, and the top quark is measured for the first time in p-p collisions. Many more exciting results are expected in the coming months.

References

[1] J.M. Campbell, J.W. Huston and W.J. Stirling, *Hard interactions of quarks and gluons: a primer for LHC physics*, Rep. Prog. Phys. **70** (2007).

[2] The CMS Collaboration, JINST 3 (2008) S08004.

[3] The CMS Collaboration, *Measurement of CMS Luminosity*, CMS-PAS-EWK-10-004 (2010).

[4] M. Cacciari, G. P. Salam, and G. Soyez, *The anti-kt jet clustering algorithm*, JHEP **04** p.63 (2008).

[5] The CMS Collaboration, *Jet Performance in pp Collisions at 7 TeV*, CMS-PAS-JME-10-003 (2010).

[6] The CMS Collaboration, *The Jet Plus Tracks Algorithm* , CMS-PAS-JME-09-002 (2009).

[7] The CMS Collaboration, *Commissioning of Particle-Flow*, CMS-PAS-PFT-10-002 (2010).

[8] The CMS Collaboration, *Commissioning of TrackJets*, CMS-PAS-JME-10-006 (2010).

[9] The CMS Collaboration, *CMS MET Performance* , CMS-PAS-JME-10-005 (2010).

[10] The CMS Collaboration, *Measurement of the Inclusive Jet Cross Section*,CMS-PAS-QCD-10-011 (2010).

[11] The DØ Collaboration, *Measurement of the inclusive jet cross section in $p\bar{p}$ collisions at $\sqrt{s} = 1.96$TeV*, Phys. Rev. Lett. **101** p.62001 (2008).

[12] T. Kluge, K. Rabbertz, M. Wobisch, *Fast pQCD calculations for PDF fits*, hep-ph/0609285 (2006).

[13] The CMS Collaboration, *Search for Quark Compositeness with the Dijet Centrality Ratio in pp Collisions at $\sqrt{s} = 7$ TeV*, CERN-PH-EP-2010-038, *Search for Dijet Resonances in 7 TeV pp Collisions at CMS*, CERN-PH-EP-2010-035 (2010).

[14] The CMS Collaboration, *Measurement of the 3-jet to 2-jet Ratio*, CMS-PAS-QCD-10-012 (2010).

[15] The CMS Collaboration, *Electron reconstruction and identification*, CMS-PAS-EGM-10-004 (2010).

[16] The CMS Collaboration, *Performance of muon identification*, CMS-PAS-MUO-10-002 (2010).

[17] The CMS Collaboration, *Inclusive Upsilon production cross section*, CMS-PAS-BPH-10-003 (2010).

[18] The CMS Collaboration, *W and Z inclusive production cross sections*, CMS-PAS-EWK-10-002 (2010).

[19] The CMS Collaboration, *Study of tau reconstruction algorithms*, CMS-PAS-PFT-10-004 (2010).

[20] The CMS Collaboration, *First Measurement of the Cross Section for Top-Quark Pair Production in Proton-Proton Collisions at $\sqrt{s} = 7$ TeV*, CERN-PH-EP-2010-039 (2010).

[21] The CMS Collaboration, *Commissioning of b-jet identification*, CMS-PAS-BTV-10-001 (2010).